Geant4-DNA example applications for track structure simulations in liquid water

A report from the Geant4-DNA Project

Incerti, S.; Kyriakou, I.; Bernal, M. A.; Bordage, M. C.; Francis, Z.; Guatelli, S.; Lee, S. B.; Tang, N.; Tran, H. N.; Brown, J. M.C.

DOI
10.1002/mp.13048

Publication date
2018

Document Version
Final published version

Published in
Medical Physics

At home. On site.
In sync.

SunCHECK™ enables complete, collaborative **remote QA coverage** for COVID-19 & beyond.

Click to explore:

- Advantages of a centralized Patient & Machine QA solution
- How SunCHECK eased the transition to remote work for users worldwide
- Three new ways we're simplifying Platform adoption

Go to: **sunnuclear.com/getprepared**

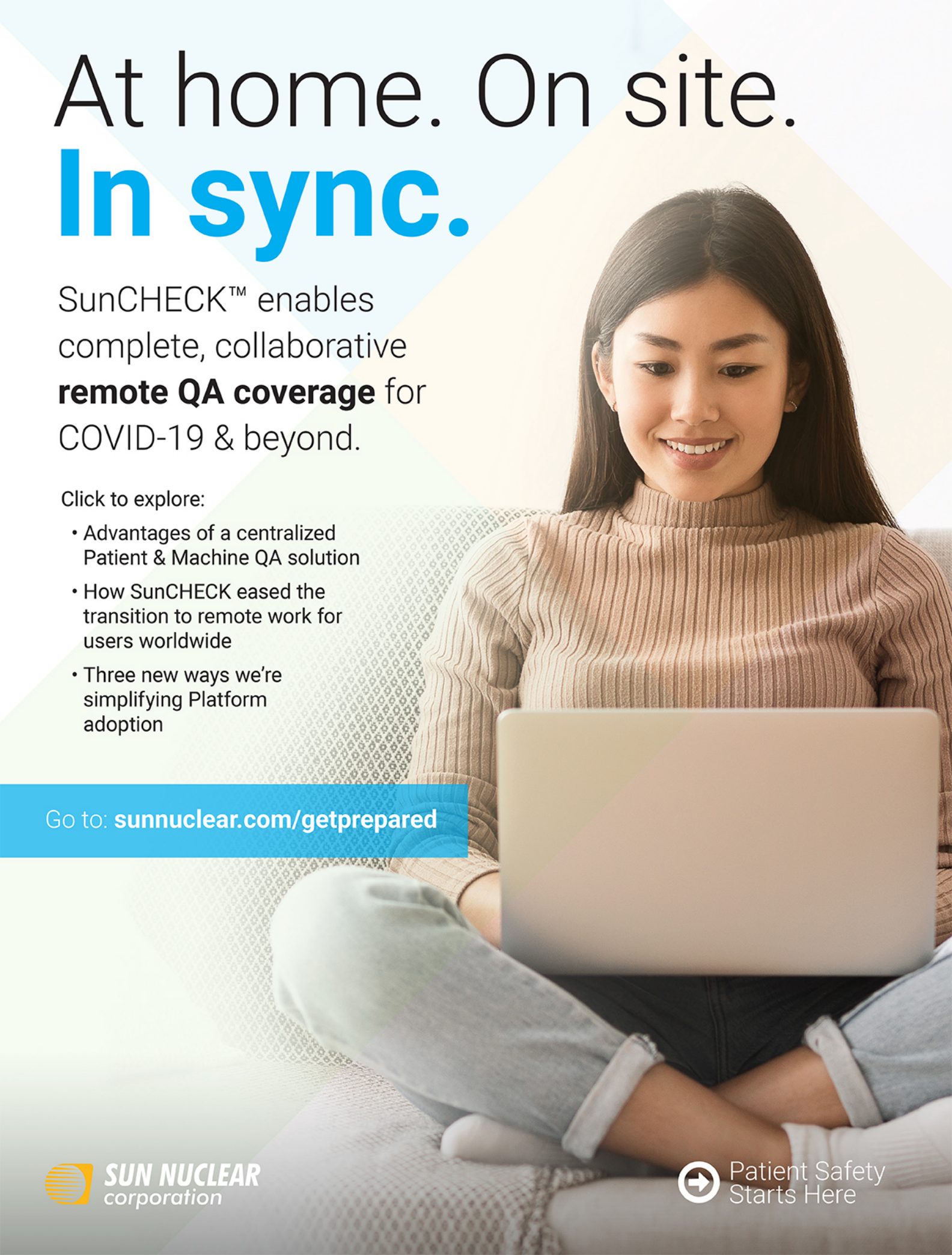

SUN NUCLEAR corporation

Patient Safety Starts Here

Geant4-DNA example applications for track structure simulations in liquid water: A report from the Geant4-DNA Project

S. Incerti[a)]
University of Bordeaux, CENBG, UMR 5797, F-33170 Gradignan, France
CNRS, IN2P3, CENBG, UMR 5797, F-33170 Gradignan, France

I. Kyriakou
Medical Physics Laboratory, University of Ioannina Medical School, 45110 Ioannina, Greece

M. A. Bernal
Instituto de Física Gleb Wataghin, Universidade Estadual de Campinas, Campinas, SP, Brazil

M. C. Bordage
Université Toulouse III-Paul Sabatier, UMR1037 CRCT, Toulouse, France
Inserm, UMR1037 CRCT, Toulouse, France

Z. Francis
Department of Physics, Faculty of Sciences, Université Saint Joseph, Beirut, Lebanon

S. Guatelli
Centre for Medical Radiation Physics, University of Wollongong, Wollongong, Australia
Illawarra Health & Medical Research Institute, University of Wollongong, Wollongong, Australia

V. Ivanchenko
Geant4 Associates International Ltd., Hebden Bridge, UK
Tomsk State University, Tomsk, Russia

M. Karamitros
Radiation Laboratory, University of Notre Dame, Notre Dame, IN 46556, USA

N. Lampe
Vicinity Centres, Data Science & Insights, Office Tower One, 1341 Dandenong Rd, Chadstone, Victoria 3148, Australia

S. B. Lee
Proton Therapy Center, National Cancer Center, 323, Ilsan-ro, Ilsandong-gu, Goyang-si, Gyeonggi-do, Korea

S. Meylan
SymAlgo Technologies, 75 rue Léon Frot, 75011 Paris, France

C. H. Min, and W. G. Shin[*,#]
Department of Radiation Convergence Engineering, Yonsei University, Wonju, Korea

P. Nieminen
ESA-ESTEC, Noordwijk, The Netherlands

D. Sakata
Centre for Medical Radiation Physics, University of Wollongong, Wollongong, Australia
University of Bordeaux, CENBG, UMR 5797, F-33170 Gradignan, France
CNRS, IN2P3, CENBG, UMR 5797, F-33170 Gradignan, France

N. Tang, and C. Villagrasa
IRSN, Institut de Radioprotection et de Sureté Nucléaire, 92262 Fontenay-aux-Roses, France

H. N. Tran
Division of Nuclear Physics, Advanced Institute of Materials Science, Ton Duc Thang University, Ho Chi Minh City, Vietnam
Faculty of Applied Sciences, Ton Duc Thang University, Ho Chi Minh City, Vietnam

J. M. C. Brown
Department of Radiation Science and Technology, Delft University of Technology, Delft, The Netherlands

(Received 8 February 2018; revised 3 May 2018; accepted for publication 4 June 2018; published 12 July 2018)

This Special Report presents a description of Geant4-DNA user applications dedicated to the simulation of track structures (TS) in liquid water and associated physical quantities (e.g., range, stopping power, mean free path. . .). These example applications are included in the Geant4 Monte Carlo toolkit and are available in open access. Each application is described and comparisons to recent international recommendations are shown (e.g., ICRU, MIRD), when available. The influence of physics models available

in Geant4-DNA for the simulation of electron interactions in liquid water is discussed. Thanks to these applications, the authors show that the most recent sets of physics models available in Geant4-DNA (the so-called "option4" and "option 6" sets) enable more accurate simulation of stopping powers, dose point kernels, and W-values in liquid water, than the default set of models ("option 2") initially provided in Geant4-DNA. They also serve as reference applications for Geant4-DNA users interested in TS simulations. © *2018 American Association of Physicists in Medicine* [https://doi.org/10.1002/mp.13048]

Key words: dosimetry, Geant4-DNA, liquid water, Monte Carlo, track structure

1. INTRODUCTION

Significant progress has been achieved during the last decades for the development of accurate computational tools capable of simulating mechanistically the passage of radiation through biological matter, especially through the DNA of cell nucleus, which is still considered as the main sensitive site to ionizing radiation in cells. This progress is particularly motivated by the need for accurate treatment planning tools for proton/ion-based radiotherapy and for better estimation of the risk to human health during long duration exposure to ionizing radiation in manned space missions. Several simulation platforms have been developed so far and are still being extended today by various groups,[1] including the state-of-the-art PARTRAC[2] and KURBUC codes,[3] which are able to simulate direct and nondirect damage to DNA, including biological repair. Unfortunately, none of them is currently openly accessible to users, preventing from their large-scale usability and adaptability to various user needs.

Alternatively, the Geant4-DNA Project[4–6] (http://geant4-dna.org) proposes the first open access software framework for the simulation of ionizing radiation early biological damage at the DNA scale. It is developed by the "Geant4-DNA" Collaboration, which was officially created in 2008. The Geant4-DNA software is an extension to the Geant4 (http://geant4.org) general purpose Monte Carlo toolkit.[7–9] It is entirely included in Geant4 and can be used to simulate step by step physical interactions of particles (electrons, protons, neutral hydrogen, alpha particles including their charged states, and a few ions) down to very low energies (~10 eV) in liquid water and DNA constituents (Adenine, Thymine, Guanine, Cytosine, and backbone[10]), thanks to a variety of physics models. It also enables simulation of the physico-chemical and chemical stages of water radiolysis in the irradiated medium up to 1 μs after irradiation,[11] and benefits from the Geant4 ability to model geometries of various biological targets at the micrometer and nanometer scale.[12] We recently demonstrated the combination of the simulation of physical, physico-chemical, and chemical interactions with such geometries in order to predict direct and nondirect early DNA damage induction in simplified models of bacterial cells[13–15] and human fibroblasts.[16] Such early damage predictions require an accurate modeling of the track structures of particles in the biological medium.[17–19]

Over the last decades, the application of Monte Carlo radiation transport modeling in the field of radiobiology has seen a distinct shift in applicable scale from tissue (millimeter)[20,21] to cellular (micron)[22,23] and, more recently, subcellular (nanometer)[24–26] investigations. To ensure the accuracy at these new length scales of interest, it is important to simulate secondary electrons down to the excitation (or ionization) threshold of the medium, which is in the 7–10 eV range for liquid water. Taking into account the details provided by the simulations, radiation quality, and the size of the target to be studied, Monte Carlo codes can be generally classified as condensed history (CH) or track structure (TS) codes.[27] CH codes group many physical interactions together, speeding up the simulation while reducing the spatial accuracy of local energy deposition. They use multiple scattering theories and stopping power data to be applicable to many materials. Codes such as EGS,[28] Geant4,[7–9] PENELOPE,[29] MCNP,[30] and FLUKA,[31] employ the CH technique and are called general purpose Monte Carlo codes because they can be utilized for a variety of applications usually from the keV up to the GeV-TeV energy range, spanning from high-energy physics, to medical physics and space radiation applications. Some of these codes, including Geant4, offer a mixed approach which enables separate treatment of "soft" and "hard" collisions, with the latter being simulated in a single-scattering mode. Despite the improved spatial resolution offered by mixed CH simulations, their application to low-energy (sub-keV) electrons may result in artifacts due to the nature of their physical models which are largely based on high-energy approximations and a combination of different theories.[32] TS codes provide a detailed treatment of all interactions using single-scattering models and thus they offer the appropriate spatial resolution for small biological targets. TS simulations are widely recognized as the preferred approach for micro- and, especially, nano-dosimetry. Several TS codes for radiobiological applications have been developed, with notable examples being the NOREC,[33] PARTRAC,[34] and KURBUC[35] codes, among others.[27] Recently, the implementation of sophisticated DNA damage and repair pathways in TS codes has been illustrated.[36,37] A few popular general purpose Monte Carlo codes such as PENELOPE[32] and MCNP (version 6[38]) also propose TS simulation capabilities down to low energies (50 and 10 eV, respectively).

During the last decade, Geant4-DNA has been equipped with a variety of physics models for the simulation of electron interactions in liquid water enabling Geant4 to perform TS simulations for biological targets. Being fully included in Geant4, these TS simulation capabilities are also accessible via user-friendly wrapper tools like TOPAS[39] and GATE[40] which are based on Geant4. The development of such physics models is an active field of research in theoretical radiation physics[41–43] and it is currently not possible to fully validate these models in

the liquid phase of water due to a lack of experimental data.[5] Thus, instead of proposing a single unique model, Geant4-DNA offers a variety of models to simulate the physical interactions of electrons in liquid water and gives the user the freedom of choice. Interactions are grouped in three categories: elastic interactions (i.e., elastic scattering), inelastic interactions (electronic excitation and ionization), and inelastic subexcitation interactions (vibrational excitation and molecular attachment, which apply to electrons that do not have sufficient kinetic energy to undergo electronic excitation nor ionization).

In addition, Geant4-DNA provides users with examples demonstrating how to simulate key quantities regularly studied in the literature, especially for the evaluation of the accuracy of TS codes. Note that Geant4-DNA also proposes other examples[6] for the simulation of water radiolysis and for the modeling of geometries of biological targets, such as DNA, but their description is beyond the scope of this report, which focuses on (physical) TS simulations in liquid water. In Geant4, an example is a ready-to-use application which is provided with its source code distribution. Today, about 100 such examples are included in Geant4 for a variety of usages. In this work, we present for the first time an overview of the Geant4-DNA examples available to users for TS simulations in liquid water. These examples enable the simulation of a variety of key physical quantities, such as range, stopping power, mean free path, mean energy required for the creation of an ion pair (so-called "W-value"), dose to liquid water target per unit of cumulated activity in a source region ("S-value"), electron slowing-down spectra, microdosimetry distributions, and dose point kernels. Such examples are used internally on a monthly basis by the Geant4-DNA Collaboration for regression testing of the software and also serve as reference applications for teaching the usage of Geant4-DNA physics models.

2. GEANT4-DNA PHYSICS CONSTRUCTORS

Geant4-DNA, included in Geant4 version 10.4 (December 2017), currently offers three recommended reference physics constructors for the simulation of discrete particle interactions in liquid water. In Geant4, a physics constructor gathers all required lists of particles, physics processes, and associated models required by a Geant4-DNA simulation application. These constructors are referenced as "G4EmDNAPhysics_option2," "G4EmDNA Physics_option4," and "G4EmDNAPhysics_option6." These three constructors use different physics models for the simulation of electron interactions as will be described later in this section. In this work, they will be referred to as "option 2," "option 4," and "option 6" constructors, respectively. An overview of the physics processes and models included for the simulation of electron interactions in liquid water is presented in Table I.

Interactions of protons, neutral hydrogen, alpha particles and their charged states, heavier ions (^{7}Li,^{9}Be,^{11}B,^{12}C, ^{14}N,^{16}O,^{28}Si,^{56}Fe), and photons are handled identically by all three constructors. In brief, nuclear scattering is modeled through classical mechanics.[44] For protons, electronic excitation at low energy (<500 keV) is based on a velocity scaling of electron excitation cross sections (this approach is also used for hydrogen, and for alpha particles and their charged states) while it uses the Born and Bethe theories at higher energies.[5] Proton ionization uses a semi-empirical approach at low energy (<500 keV) while it is based on the Born and Bethe theories and the dielectric formalism for liquid water above this energy.[5] This semi-empirical approach is also used for hydrogen, alpha particles and their charged states, and heavier ions (note that only the ionization process is currently simulated for these heavier ions). Electron capture and electron loss are described by analytical parametrizations based on experimental data in the vapor phase. The ionization process for heavy ions uses a speed scaling of proton ionization cross section and incorporates the effective charge to take into account the screening of shell electrons.[45] Finally, photon interactions include photoelectric effect, Compton scattering, Rayleigh scattering, and pair production, and they are based on the Evaluated Photon Data Library set of models of Geant4.[46] The further detailed description of these models is already available in the literature.[5,6,44,45,47–50] In Table I we provide a summary of each Geant4-DNA physics model for electron TS simulations with emphasis on their differences.

2.A. The "Option 2" constructor (default models)

"Option 2" is the first set of discrete physics models implemented in Geant4 for electron transport in liquid water down to eV energies. Since its public release in Geant4 version 9.1 in 2007, it has been the default set of electron models in Geant4-DNA. The inelastic cross sections for the individual ionization and excitation channels of the weakly bound electrons of liquid water are calculated numerically from the complex dielectric response function, $\varepsilon(E,q) = \varepsilon_1(E,q) + \varepsilon_2(E,q)$, of the medium with E and q being the energy- and momentum transfer:

$$\sigma_{n,k} = \int \frac{d\sigma_{n,k}}{dE}\, dE = \frac{1}{\pi a_0 N T} \int dE \int \frac{\mathrm{Im}[\varepsilon_{n,k}(E,q)]}{|\varepsilon(E,q)|^2}\, \frac{dq}{q} \tag{1}$$

where σ is the inelastic cross section, a_0 is the Bohr radius, N is the density of water molecules, T is the electron kinetic energy, and the subscripts n, k denote the ionization shells and excitation levels, respectively. The imaginary part of the dielectric function at the optical limit ($q = 0$), is partitioned to four ionization shells ($1b_1$, $3a_1$, $1b_2$, $2a_1$) and five discrete electronic excitations (A^1B_1, B^1A_1, Ryd A+B, Ryd C+D, diffuse bands) according to the parameterization of Emfietzoglou[54]:

$$\begin{aligned}\mathrm{Im}[\varepsilon(E,q=0)] &= \sum_{n=1}^{4} [D_n(E;E_n)\Theta(E-B_n)] \\ &\quad + \sum_{k=1}^{5} [D_k^*(E;E_k)\Theta(E-B_k)]\end{aligned} \tag{2}$$

where $D_n(E;E_n)$ and $D_k^*(E;E_k)$ are the ordinary and derivative Drude functions with coefficients determined by a fit to optical data under the constraint of the f-sum-rule, and $B_{n,k}$

TABLE I. Content of the three reference Geant4-DNA physics constructors for TS simulations of electrons in liquid water available in the Geant4 10.4 release. Processes and models are indicated as well as their energy range of applicability and main reference. Processes are identified as elastic, inelastic, and inelastic subexcitation processes. Auger emission is listed as a separate process. We also indicate the tracking cut below which the tracking of electrons is stopped and their remaining kinetic energy is locally deposited. (*): This tracking cut is handled by a specific Geant4-DNA process — so-called "G4DNAElectronSolvation" — which does not apply when chemistry simulation is activated (electrons are tracked till thermalization and are considered as solvated).

	Geant4-DNA physics constructors electron models		
Process	G4EmDNAPhysics_option2	G4EmDNAPhysics_option4	G4EmDNAPhysics_option6
Ionization (inelastic)	Emfietzoglou dielectric model (11 eV–1 MeV)[5]	Emfietzoglou–Kyriakou dielectric model (10 eV–10 keV)[47]	Relativistic binary encounter Bethe model from CPA100 code (11 eV–256 keV)[48]
Electronic excitation (inelastic)	Emfietzoglou dielectric model (9 eV–1 MeV)[5]	Emfietzoglou–Kyriakou dielectric model (8 eV–10 keV)[47]	Dielectric model from CPA100 code (11 eV–256 keV)[48]
Elastic scattering (elastic)	Partial wave model (7.4 eV–1 MeV)[5]	Uehara screened Rutherford model (9 eV–10 keV)[47]	Independent Atom Method model from CPA100 code (11 eV–256 keV)[48]
Vibrational excitation (inelastic subexcitation)	Sanche data (2 eV–100 eV)[49]	n/a	n/a
Attachment (inelastic subexcitation)	Melton data (4 eV–13 eV)[50]	n/a	n/a
Auger electron emission	From the EADL database[51] and the Geant4 atomic relaxation interface[52,53]		
Default tracking cut(*)	7.4 eV	10 eV	11 eV

are threshold energies (e.g., binding energies). The role of the step-functions is to truncate the nonphysical contribution of the Drude functions below the threshold values of the corresponding inelastic channels. The real part of the dielectric function is obtained from Eq. (2) using the Kramers–Kronig relation. Extension of the optical dielectric function, $\varepsilon(E, q = 0)$, to $q \neq 0$ is made by semi-empirical dispersion relations for the Drude coefficients.[55] Below a few hundred eV, the first Born approximation is not directly applicable; a kinematic Coulomb-field correction and Mott-like exchange-correction terms are used.[55] Total and differential cross sections for electron-impact ionization of the K-shell (of the oxygen atom) are calculated analytically from the Binary-Encounter-Approximation-with-Exchange model (BEAX).[56] This is an atomic model which depends only upon the binding energy, mean kinetic energy, and occupation number of the orbital. The scattering angle of the primary electron and the ejection angle of the secondary electron in ionization events are determined from the kinematics of binary collisions. No angular deflection is considered in collisions leading to electronic excitation. The elastic cross sections are based on partial wave calculations, considering a total interaction potential which takes into account a static contribution as well as fine effects, like exchange and polarization contributions.[57] No energy loss is considered to take place in elastic collisions. Finally, the "option 2" constructor also takes into account the vibrational excitation and electron attachment processes which apply to electrons with kinetic energy lower than the lowest excitation level of liquid water (8.22 eV). The corresponding models have been derived from experimental data in ice (for vibrational excitation) and vapor phase (for attachment).[58] These two processes are required for the simulation of electron transport down to thermalization and subsequent water radiolysis[6] (not discussed in this work).

The "option 2" constructor contains the first set of models that were proposed in Geant4-DNA for the modeling of electron interactions in liquid water. However, we recently reported[47] some deficiencies of the default inelastic models due to the truncation of the Drude functions through the step-functions included in Eq. (2). Specifically, Eq. (2) results in the violation of the f-sum-rule, while the expression for $\mathrm{Re}[\varepsilon(E, q)]$ obtained from $\mathrm{Im}[\varepsilon(E, q)]$ via the Kramers–Kronig relation becomes nontrivial. These deficiencies triggered the development of the new "option 4" set of models, as described in the next paragraph.

2.B. The "Option 4" constructor (Ioannina models)

Since Geant4 version 10.2 released in 2016, "option 4" offers alternative discrete physics models to "option 2" (default) for electron transport in liquid water in the 10 eV–10 keV energy range. "Option 4" (developed at the University of Ioannina) provides updated cross sections for electron-impact excitation and ionization in liquid water, and an alternative elastic scattering model.[47,59,60] Similar to "option 2", inelastic cross sections are calculated from Eq. (1) using the Drude parameterization of $\varepsilon(E, q)$ by Emfietzoglou.[54] Although more advanced dielectric functions are available,[42,61] the main advantage of keeping the Drude representation in "option 4" is that due to the mathematical simplicity of the Drude functions both $\mathrm{Im}[\varepsilon(E, q)]$ and $\mathrm{Re}[\varepsilon(E, q)]$ can be expressed analytically and the f-sum-rule is fulfilled for all q regardless of the form of the dispersion relations. The deficiencies related to the truncation of the Drude functions in "option 2" are overcome in "option 4" through the replacement of Eq. (2) by the following expression[47]:

$$\begin{aligned}&\mathrm{Im}[\varepsilon(E,q=0)]\\&=\sum_{n=1}^{4}\{[D(E;E_n)-D(E;B_n)\exp(B_n-E)+F_n(E)]\Theta(E-B_n)\}\\&\quad+\sum_{k=1}^{5}\{[D_k^*(E;E_k)+F_k(E)]\Theta(E-B_k)\}\end{aligned}\tag{3}$$

where $D(E; B_n)$ exp $(B_n - E)$ is an exponential smoothing function for ionizations, and $F_{n,k}(E)$ are contributions due to the smoothing and truncation of Drude functions at higher energy-levels. The $F_{n,k}(E)$ are calculated analytically by a redistribution of the oscillator strength in a physically motivated and f-sum-rule constrained manner.[47] It must be noted that the above modifications have also been used in a recent expression of the dielectric function for liquid water which includes exchange-correlation effects that bring better agreement with the experimental data.[62] Despite starting from essentially the same optical-data model for $\varepsilon(E, q)$ with "option 2", substantially different ionization and excitation cross sections are obtained in "option 4". For example, excitations are strongly enhanced relative to ionizations (which decrease only moderately), resulting in higher mean energies required for the creation of an ion pair in liquid water (the so-called "W-values"), smaller penetration distances, and less diffused dose point kernels at sub-keV electron energies.[59] In addition, methodological changes are made in the application of the Coulomb and Mott corrections which result in more accurate ionization cross sections, especially at energies near the binding energies. These Born corrections account for most of the exchange effects on electron–electron interactions.[63,64] Finally, the elastic cross sections are calculated analytically from the screened Rutherford formula using the screening parameter of Uehara et al.[65] which is deduced from a fit to experimental data for water vapor. The screened Rutherford formula becomes inaccurate at very low energies and the Brenner–Zaider parametric expression is adopted below 200 eV which fits experimental data in the vapor phase.[59] In the absence of elastic scattering data in liquid water, it is not possible to fully validate such elastic cross sections for the liquid phase. The influence of the water phase at low impact energy is, however, expected to be small.[66]

2.C. The "Option 6" constructor (CPA100 models)

Since Geant4 version 10.4, released in 2017, "option 6" is yet another alternative set of discrete physics models for electron transport in liquid water over the 11 eV–256 keV energy range. "Option 6" is an implementation of the interaction cross sections of the CPA100 track structure code to Geant4-DNA.[48] CPA100 was developed and maintained by M. Terrissol et al.[67] and it is one of the few TS codes that can also simulate liquid water radiolysis, such as PARTRAC and KURBUC, among others.[27] The porting of CPA100 to Geant4-DNA enables easy access to these models and further expands their applicability through combination with existing Geant4 functionality (e.g., modeling of complex geometries). Regarding the modeling of track structures, cross sections for electronic excitations are calculated in the first Born approximation using the optical-data model of $\varepsilon(E, q)$ developed by Dingfelder and co-workers.[68] This model is also based on a Drude representation of $\varepsilon(E, q)$, using the same optical dataset, electronic excitation levels, and dispersion relations as "option 2" and "option 4". The resulting excitation cross sections, however, are not the same due to a different set of Drude coefficients. The ionization cross sections for the five shells of water are calculated from the Binary-Encounter-Bethe (BEB) model.[69] Thus, total and differential ionization cross sections are calculated analytically. Similar to the BEAX model used in "option 2" and "option 4" for electron-impact ionization of K-shell, the BEB model is an exchange-corrected atomic model which depends only upon the binding energy, mean kinetic energy, and occupation number of the orbital. Angular deflections in both ionization and excitation collisions are considered based on the kinematics of binary collisions. Elastic scattering cross sections are based on partial wave calculations using the independent atom approximation and very small energy loss is taken into account during each single elastic scattering.[48]

2.D. Other constructors

All the results presented in this work have been obtained using the "option 2," "option 4," and "option 6" constructors. Other physics constructors have been provided historically with Geant4-DNA. These options are either nonvalidated (such as "option 1"), obsolete ("option 3") or accelerated versions of other options for faster computing (e.g., "option 5" is an alternative of "option 4"). "G4EmDNAPhysics" is the default constructor initially delivered to Geant4 in December 2007. This constructor proposes slower versions of the elastic scattering and ionization processes than the "option 2" constructor, by using noncumulated differential cross sections for the description of the physical interactions (calculation of scattering angle for elastic scattering and calculation of secondary electron kinetic energy for ionization); instead "option 2" uses the cumulated version of these differential cross sections. The "G4EmDNAPhysics_option1" constructor uses the "G4LowEWentzelVI" model[70] for the simulation of electron elastic scattering, which is a low-energy extension of the original "WentzelVI" elastic scattering model described in Ref. [71]. Although faster, this model has not been validated compared to existing Geant4-DNA elastic single-scattering models and experimental data and is currently provided as a beta development only. The "G4EmDNAPhysics_option3" constructor is obsolete. The "G4EmDNAPhysics_option5" constructor provides an accelerated version of the "option 4" constructor. However, since the energy applicability of "option 4" is currently limited to 10 keV, this constructor can be used for TS simulations without a strong computing performance penalty while keeping the accuracy of noncumulated differential cross sections. With the future evolution of the electron ionization model currently available in "option 4", the usage of "option 5" might become an interesting

TABLE II. List of Geant4-DNA "extended" examples available for TS simulations in liquid water. These examples are available in Geant4 release 10.4 (December 2017). The Geant4-DNA macro files used to obtain most of the results presented in this work are given. Other related references are indicated as well. (+): These examples are not specific to Geant4-DNA but are equipped with Geant4-DNA macro files for TS simulations.

Extended example name	Purpose	Macro file	Other related reference(s)
dnaphysics	Detail of tracking, automatic combination with Geant4 standard EM physics models, modification of medium density	dnaphysics.in	[6]
microdosimetry	Combination "by hand" of Geant4 standard EM and Geant4-DNA processes and models in different regions	microdosimetry.in	[6]
range	Range, projected range, penetration	range.in	[59]
spower	Stopping power	spower.in	[72]
mfp	Mean free path	mfp.in	–
wvalue	Mean energy required for the creation of an ion pair in liquid water (the so-called "W-value")	wvalue.in	[47]
svalue	Dose to a liquid water target per unit of cumulated activity in a source region (the so-called "S-value")	svalue.in	[6,73,74]
slowing	Slowing-down electron spectra	slowing.in	[72]
microyz	Microdosimetric distributions (lineal energy y, specific energy z) and related quantities	microyz.in	[60]
TestEm12(+)	Dose point kernel	dna.mac	[6,59,75]
TestEm5(+)	Identification of atomic de-excitation products for Geant4-DNA processes	dna.mac	–

alternative. Finally, an *ad hoc* constructor is proposed as "G4EmDNAPhysics_option7", combining "option 4" electron models (up to 10 keV) and default Geant4-DNA electron models (from 10 keV up to 1 MeV). This combination is now available through a new software interface ("G4EmDNAPhysicsActivator"), which offers in particular the possibility to track electrons above 1 MeV using Geant4 standard electromagnetic processes and models. This feature will be described later in this work.

3. GEANT4-DNA EXAMPLES FOR TS SIMULATIONS IN LIQUID WATER

Geant4-DNA currently provides 11 examples that can be used to simulate track structures in liquid water. These examples belong to the so-called "extended" category of examples available in the Geant4 toolkit, in parallel to the general "novice" and "advanced" categories of examples which are also available in Geant4. They are all located in the "examples/extended/medical/dna" directory of the toolkit. The list of these examples is summarized in Table II.

We describe below the main features proposed by these examples, starting from more fundamental examples to a variety of applications. These examples will serve as reference applications for users who have interest in simulating quantities described in Table II, which are frequently used in TS simulations. We also present and discuss for each example the performance of the three Geant4-DNA physics constructors ("option 2," "option 4," and "option 6") for the simulation of these quantities.

All examples are provided with Geant4 macro files. These macro files are text files which contain Geant4 commands allowing an easy control of the simulation and associated settings, without the need for recompilation of the user application. The names of these macro files are listed in Table II. Some of the examples also include ROOT[76] macro files for the automatic generation of graphs. These macros contain C++ commands which are directly interpreted by ROOT. The results presented in this work have been obtained exclusively from the described examples, run on a laptop computer equipped with the Geant4 virtual machine (http://geant4.in2p3.fr) developed at CENBG. These examples can be run in multithreading mode, which allows an optimized usage of cores and memory in recent computers.[9] The virtual machine contains the full Geant4 installation, ROOT, and other tools, and is freely available for download.

3.A. The "dnaphysics" example

3.A.1. Purpose

Historically, the "dnaphysics" example was the first example offered to users illustrating the usage of Geant4-DNA physics processes and models for the simulation of TS in liquid water. This example allows the scoring of all step by step information of particle tracking in liquid water including physical interaction process (e.g., ionization, electronic excitation...), step position (the so-called pre- and poststep points of each step), local energy deposition, step size, kinetic energy loss, scattering angle, and track hierarchy (i.e., identification of current step, current track, and parent track).

This example illustrates the usage of the new "G4EmDNAPhysicsActivator" interface available in Geant4 since release 10.4. This interface performs the automatic combination of Geant4-DNA models and Geant4 electromagnetic physics models in a geometrical region of the simulated setup specified by the user. This allows, for example, to simulate the interactions of electrons beyond the 1 MeV maximum

upper limit of Geant4-DNA electron models (available in the "option 2" constructor) using Geant4 electromagnetic physics models above this limit. In the current implementation of this interface, Geant4 electromagnetic physics models are taken from the "G4EmStandardPhysics_option4" standard electromagnetic physics constructor of Geant4.[9] Table III details the current combination of electron models proposed by this new interface (the combination for other Geant4-DNA particles, including photons, is described in the Supporting Information Table S1).

This new interface can be used in any application directly via User Interface commands and does not require any coding of a combined physics list. Such a combination between Geant4-DNA and Geant4 models, which is not straightforward, was initially demonstrated in the Geant4-DNA "microdosimetry" example[6] where a reference physics list was constructed for users wishing to build their own combination of Geant4-DNA models with Geant4 electromagnetic physics models. This "microdosimetry" example is now kept for preservation.

Alternatively, users can choose to select exclusively any of the Geant4-DNA physics constructors for the tracking of particles. The simulation of atomic relaxation (production of Auger electrons and fluorescence photons[52]) is enabled as well. Atomic relaxation is triggered when ionization of water K-shell occurs. Corresponding transition probabilities and emission energies from oxygen atom are taken from the Evaluated Atomic Data Library (EADL) atomistic database[51] similarly to Geant4 ionizing electromagnetic processes, as we recently detailed in Ref. [52, 53].

The variable density feature of Geant4 materials is also illustrated by this example: this is an easy way to use the same Geant4-DNA cross sections for a liquid water medium having a density different than the default NIST value used by Geant4-DNA models (i.e., 1 g/cm^3). For example, the state-of-the-art PARTRAC damage simulation software uses a value of 1.06 g/cm^3 for liquid water to approximate cell constituents.[78]

TABLE III. Description of the automatic combination of Geant4-DNA models with Geant4 standard electromagnetic models for electrons in liquid water, performed by the "G4EmDNAPhysicsActivator" interface available from Geant4 10.4 release (December 2017), and illustrated in the "dnaphysics" example.

Physical process	Geant4-DNA electron model	Geant4 electron standard electromagnetic model
Elastic	Partial wave (<1 MeV)	Urban (multiple scat., > 1 MeV) or Coulomb (single scat., > 1 MeV)
Electronic excitation	Emfietzoglou–Kyriakou (<10 keV) and default (10 keV–1 MeV)	n/a
Ionization	Emfietzoglou–Kyriakou (<10 keV) and default (10 keV–1 MeV)	Moller–Bhabha (>1 MeV)
Vibrational excitation	Sanche (<100 eV)	n/a
Attachment	Melton (<13 eV)	n/a

3.A.2. Results and discussion

This example can be utilized to study physical processes occurring along particle tracks. As an example, Fig. 1 shows the frequency of Geant4-DNA physics processes for 10^2 protons with energy 100 keV, incident in an infinite volume of liquid water. The default Geant4-DNA tracking cut for protons and hydrogen atoms was used (100 eV). The results are presented for the three Geant4-DNA physics constructors, alternatively adopted to describe the particle interactions (note that larger statistics lead to the same observations). The histograms of Fig. 1 are automatically generated by the ROOT macro provided with the example. As can be observed from Fig. 1, Geant4-DNA physics processes for protons and hydrogen atoms occur with similar frequencies for the three physics constructors. These constructors indeed differ only by the models used to describe electrons interactions, as summarized in Table I. Figure 1 also illustrates that for the case of the default constructor ("option 2"), vibrational excitation and molecular attachment are activated, while these two processes are not considered by the two other constructors ("option 4" and "option 6"). "Option 2" and "option 6" generate more ionizations than "option 4", which in turn generates more electronic excitations, because of the larger contribution of the excitation cross section, as explained in Ref. [47]. Finally, elastic scattering occurs more frequently in "option 2", since electrons are transported down to 7.4 eV (they are transported down to 10 or 11 eV, for "option 4" or "option 6", respectively — see Table I).

We provide in Supporting Information Fig. S1 a visual comparison of three tracks of particles with similar initial velocities simulated using "dnaphysics": a 1 MeV proton, a 4 MeV alpha particle and a 12 MeV carbon ion, over a distance of 500 nm in liquid water, simulated with the "G4EmDNAPhysicsActivator" interface which combines Geant4 electromagnetic physics models and Geant4-DNA physics models. We used the same color code as in Fig. 1 to mark physical interactions. This enabled us to illustrate the "cloud" of electron elastic scattering sites that surrounds the core of the incident particle track and secondary electron tracks.

3.B. The "range" example

3.B.1. Purpose

While the "dnaphysics" example allows for the easy extraction of the main physical quantities of the incident particle and the whole shower of secondary particles created during the tracking, the "range" example simulates the total distance travelled — the so-called "range" — by an incident particle.

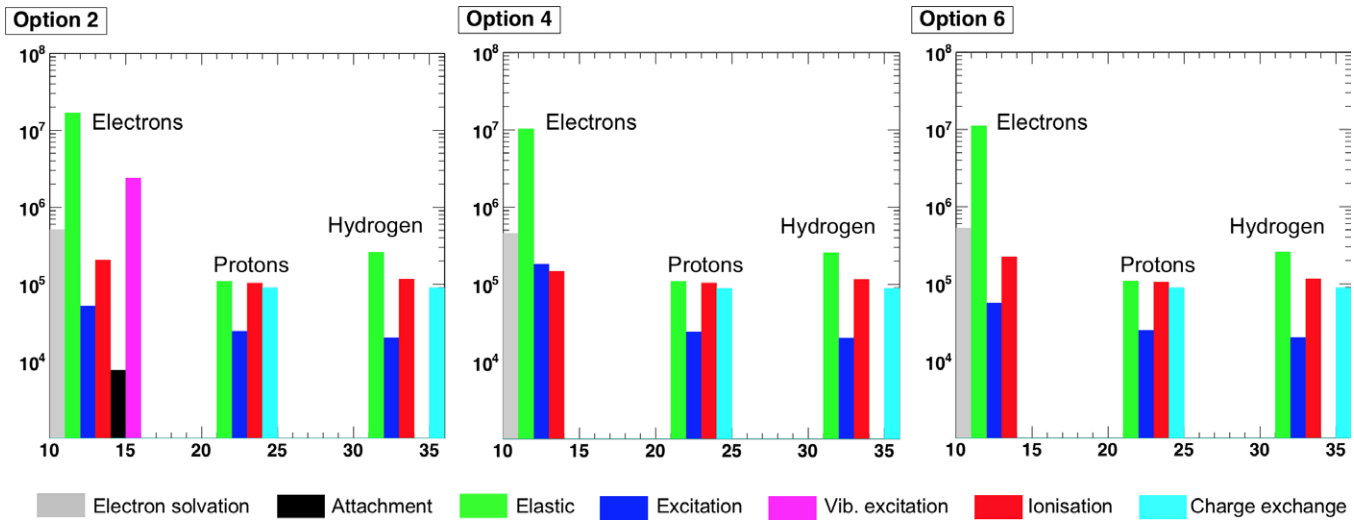

FIG. 1. Illustration of the usage of the "dnaphysics" example for the scoring of Geant4-DNA processes occurring along 10^2 incident proton tracks of 100 keV in an infinite volume of liquid water. The left plot has been obtained with Geant4-DNA physics constructor "option 2" (default models), the middle plot with "option 4" (Ioannina U. models), and the right one with "option 6" (CPA100 models). Occurrences are represented by vertical bars, as a function of particle type. The numbers indicated on the horizontal axis are used to identify processes in the application.

In this example, the "range" can be tracked until the particle reaches a minimum tracking cut, which can be set by the user, below which this particle is stopped and its remaining kinetic energy is deposited locally into the liquid water medium. In addition, two other quantities are calculated: the "penetration" which represents the distance between the point where the incident particle is shot and the point where its tracking is stopped, and the "projected range" which represents the projection of the "penetration range" along the shooting direction. Naturally, only the incident particle is considered in these simulations. Simulated values are given in nanometers. This example can serve as a benchmark against international recommendations, as we will further discuss below.

3.B.2. Results and discussion

Figure 2 shows the simulation of particle ranges, defined as the sum of all step lengths of the primary particle (electrons, protons, alphas) cumulated over the entire track length, as a function of incident energy, as simulated by the "range" example. For the calculation of electron range, the three Geant4-DNA physics constructors were used with their default tracking cut. For the calculation of proton range, a variable tracking cut has been applied following the procedure initially proposed by Uehara et al. in Ref. [80] and also used in previous Geant4-DNA comparisons.[44] Specifically, the tracking cut has been set to 400 eV at the incident kinetic energy of 1 keV, and to 3 keV at the incident kinetic energy of 500 keV, and its value is interpolated logarithmically for intermediate incident energies. For the simulation of alpha range, the low-energy limit of the ionization model was extended down to 100 eV instead of 1 keV, which is currently the default tracking cut of alpha particles in Geant4-DNA.[5] For comparison, ICRU90 ranges for liquid water are indicated as well.[79] Regarding electrons, below a few keV, "option 2" values are the largest, followed by "option 4"

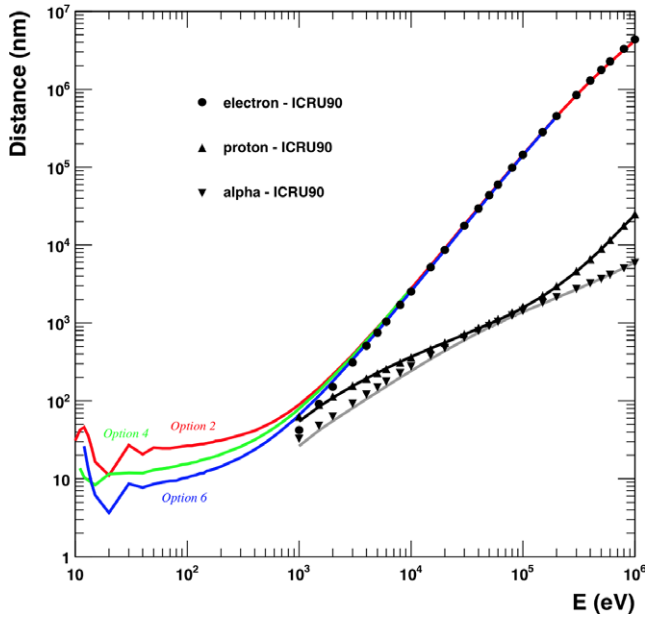

FIG. 2. Electron, proton, and alpha ranges (all represented as solid lines) in liquid water simulated using the "range" example as a function of incident kinetic energy. For electrons, results obtained for the three Geant4-DNA physics constructors are indicated (in red for "option 2," in green for "option 4," and in blue for "option 6"). Symbols represent the recent ICRU90 recommendations[79].

values which are larger than "option 6" values, the latter being closer to ICRU data. Compared to "option 4", the larger values obtained with "option 2" result mainly from the lower tracking cut proposed by the physics constructor (7.4 vs 10 eV). "Option 6" tends to predict systematically shorter ranges especially at the lowest energies. This is a consequence of the larger inelastic cross section for electrons in the 10 eV–10 keV range available in "option 6" as can be observed in Fig. 4 of Ref. [6]. The oscillations observed at

very low energy are caused by the rapidly decreasing cross sections for inelastic interactions (including vibrational excitations), as already underlined in Ref. [81] and are not due to statistical fluctuations (10^6 incident electrons were shot for this Figure). Good agreement is observed with the recent ICRU90 recommendations at high energies. Quantitatively, the simulation results start to deviate by more than 10% from ICRU90 recommendations below 10 keV for "option 2" and "option 4" and below 3 keV for "option 6". Proton ranges agree better than 5% down to 2 keV while alpha ranges deviate by more than 10% below 15 keV.

3.C. The "spower" example

3.C.1. Purpose

Similar to the "range" example, the "spower" example serves as a benchmark to international recommendations on stopping power in liquid water. Simulated values are expressed in MeV/cm for easier comparison to international recommendations. This example activates a stationary mode (frozen-velocity approximation) in models where the incident particle loses energy. In this mode, the kinetic energy of the incident particle is artificially maintained constant at each simulation step. This ensures the correct calculation of the stopping power according to its definition. Secondary particles are not transported during the simulation, and charge exchange processes (electron capture or loss) are considered for protons, hydrogen, alpha particles, and their charge states. Nuclear scattering by protons, alpha particles, and their charge states can be deactivated if the user is only interested in the simulation of the electronic stopping power.

3.C.2. Results and discussion

Figure 3 shows the simulation of particle stopping power as a function of incident energy, assuming a stationary regime, as explained in the previous section. Electron stopping powers are shown on the left plot, for the three Geant4-DNA physics constructors and on the right plot for protons and alpha particles. Regarding electrons, stopping power calculated using "option 6" is larger than "option 2" and "option 4" predictions, which is again a consequence of larger inelastic cross sections for "option 6" compared to the two other constructors (similarly, inelastic cross sections are larger for "option 2" than for "option 4", as shown by the corresponding stopping power curves). Regarding comparison to ICRU90 recommendations, Geant4-DNA predictions for electrons are compared to ICRU90 electronic stopping power. "Option 2" and "option 4" values differ from ICRU90 recommendations by 5% and less in the 4 keV–500 keV range ("option 4" does not go beyond 10 keV), and around 10% down to 1 keV. "Option 6" differs from ICRU90 by less than 4% on the whole energy range covered by this constructor; in particular, it differs by 2% and less below 4 keV down to 1 keV. We should note that ICRU90 stopping power values have a 1.5–5% uncertainty in the range of 1–10 keV. They also neglect shell-corrections which reduce the Bethe stopping power below a few keV.[82] Regarding protons, simulations differ by less than 5% from ICRU90 down to 20 keV. Finally, regarding alpha particles, the differences are larger than 10% below 10 keV and from 150 MeV.

3.D. The "mfp" example

3.D.1. Purpose

The "mfp" example simulates mean free path values. This is particularly interesting for the comparison of simulation performance of TS codes for electrons in liquid water at low energies and in small volumes, as recently outlined in Emfietzoglou et al.[83] Users can easily inactivate any Geant4-DNA process thanks to a dedicated process inactivation macro command, allowing, for example, the simulation of inelastic mean free path for electrons by having the elastic scattering process switched-off. Simulated mean free path values are expressed in nm.

3.D.2. Results and discussion

Figure 4 presents electron mean free path as a function of incident energy simulated using the three Geant4-DNA physics constructors. We indicate in these figures mean free paths simulated with all processes active (dashed lines) or with inelastic processes active only (i.e., ionization, electronic, and vibrational excitation only — solid lines). Globally, for both cases, all curves have similar tendencies. In the case where only inelastic processes are considered, mean free path values obtained with "option 6" are smaller than values simulated with "option 4", which follow "option 2" values down to 100 eV. This is a consequence of the dominance of the sum of inelastic cross sections in "option 6" compared to the two other options, as shown in Fig. 4 of Ref. [6]. At 100 eV and below, the observed step affecting "option 2" values (solid and dashed red lines) is caused by the vibrational excitation process which becomes active and induces additional energy losses, reducing the mean free path value. In the case where all processes available in physics constructors are active, "option 6" values are systematically smaller than "option 4" values, which tend to become smaller than "option 2" values with decreasing incident energy. As international recommendations (e.g., ICRU reports) for mean free path values are not available yet, it is currently not possible to draw quantitative conclusions on the verification of simulated mean free path values.

3.E. The "wvalue" example

3.E.1. Purpose

The "wvalue" example is provided in order to evaluate the accuracy of Geant4-DNA constructors for the simulation of the mean energy (the so-called "W-value") required for the

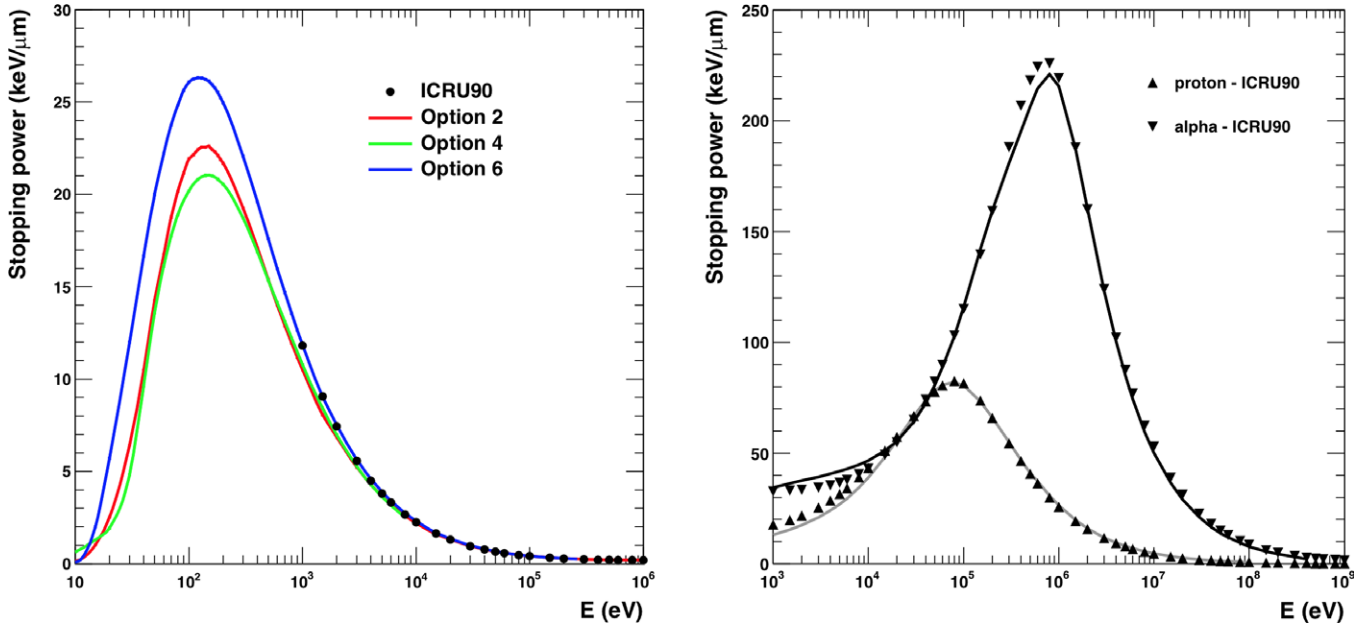

FIG. 3. Stopping power for electrons (left plot, solid lines), protons, and alpha particles (right plot, solid lines) in liquid water as a function of incident energy, simulated with the "spower" example. For electrons, results obtained for the three Geant4-DNA physics constructors are indicated (in red for "option 2," in green for "option 4," and in blue for "option 6"). Symbols represent the recent corresponding ICRU90 recommendations for stopping power (electronic stopping power on left plot, total stopping power on right plot)[79].

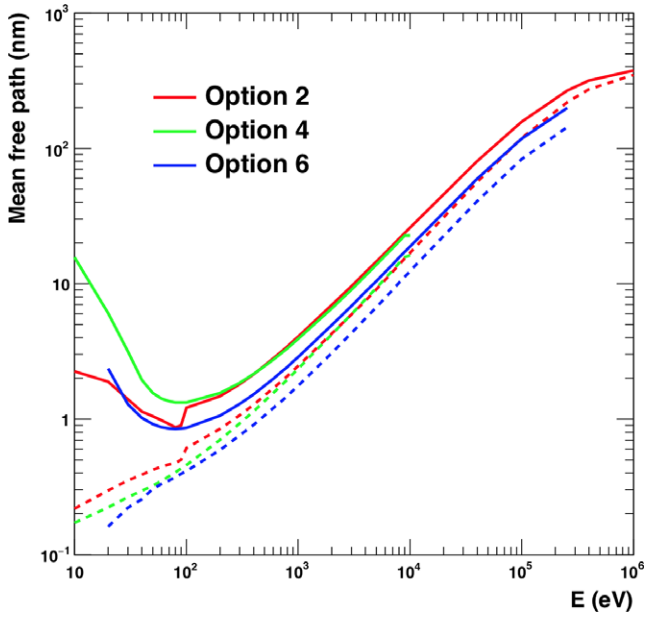

FIG. 4. Mean free path for electrons in liquid water, considering all physical interactions (dashed lines) or inelastic interactions only (solid lines) as a function of incident particle energy, simulated with the "mfp" example, for the three Geant4-DNA physics constructors.

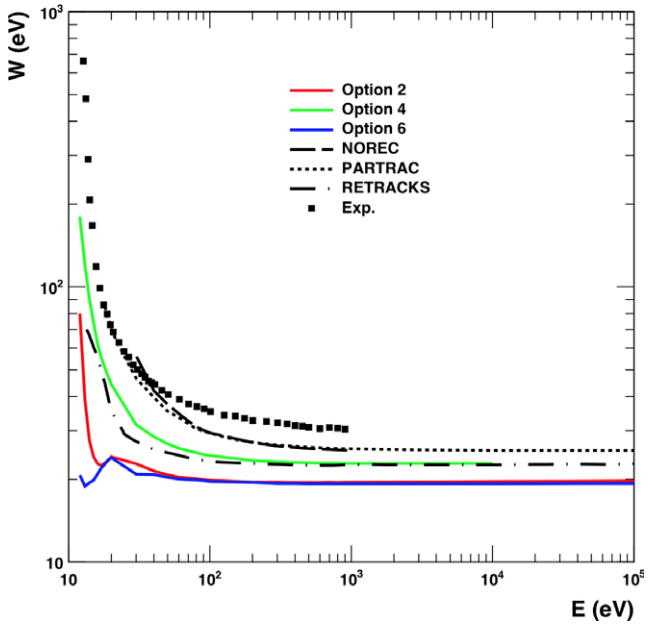

FIG 5. W-value for electrons as a function of incident energy up to 100 keV in liquid water simulated using the "wvalue" example, for the three Geant4-DNA constructors. Monte Carlo simulations from NOREC (dashed line, Ref. [33]), PARTRAC (dotted line, Ref. [33]), RETRACKS (dash-dotted line, Ref. [84]) and experimental data in gaseous water (squares, Ref. [85]) are shown as well for comparison.

creation of an ion pair in liquid water during the slowing down of an initial particle for given incident energy.[47] This is another benchmark regularly used in the literature to compare TS codes. The user has the possibility to easily select a tracking cut used for the simulation, below which the tracking of particles is stopped and their energy is locally dumped. Simulated W-values are expressed in eV.

3.E.2. Results and discussion

We present in Fig. 5 the simulation of W-values for the three Geant4-DNA physics constructors. In these simulations,

we have applied the default tracking cut of the constructors (7.4 eV for "option 2," 10 eV for "option 4," and 11 eV for "option 6"). Results are identical to the case where a common tracking cut of 11 eV was used,[47] and underline that a small change in the tracking cut does not influence the W-value. For comparison, NOREC,[33,86] PARTRAC,[33] and RETRACKS[84] simulations and experimental data in gaseous water[85] are shown as well. While "option 2" and "option 6" values remain close down to about 20 eV, "option 4" predictions are the closest to NOREC and PARTRAC simulations; they are also closer to the experimental dataset in the gaseous phase, which represents an upper bound of values in the liquid phase.[47] The observed better agreement of "option 4" compared to the two other physics constructors results from the larger ratio of excitation to ionization cross sections for this constructor.

3.F. The "svalue" example

3.F.1. Purpose

The "svalue" example allows the simulation of S-values which are (mainly) used in targeted radionuclide therapy in order to convert administered activity to radiation dose, as explained by the MIRD committee.[73,87] The S-values represent the dose to a target region per unit of cumulated activity in a source region. The most recent version of the example (which will be released in the near future) simulates the S-values for a spherical shell of liquid water surrounding a plain sphere of liquid water, representing a simplified cytoplasm and nucleus, respectively. Users may select radii and easily change component materials (e.g., liquid water or vacuum). By default, particles are emitted randomly from the cytoplasm volume, a typical configuration for radionuclide therapy in cells.[88] Three configurations can be selected for the description of incident particle emission. Monoenergetic particles are simulated by default. Alternatively, the user can provide a file containing a list of emission energies. The application is adapted to handle such a file in multithreading mode using a dedicated cache mechanism. As a third option, radionuclides, such as Iodine 125 and Iodine 131, can be set as point-like radiation sources. In this case, the radionuclide emission spectrum is directly simulated by the radioactive decay module of Geant4; two macro files are provided as examples. Any radionuclide handled by the radioactive decay module can thus be simulated. Finally, users can also select the tracking cut used in their simulation. The "svalue" example simulates by default S-values for (nucleus ← cytoplasm) and (cytoplasm ← cytoplasm) irradiation, and it can be easily adapted for any other configuration (target ← source). The simulated S-values are expressed in Gy/Bq.s.

3.F.2. Results and discussion

Figure 6 shows the simulation of S-values for a simplified biological cell, containing a spherical nucleus of radius 4 micrometer, surrounded by a spherical cytoplasm of thickness

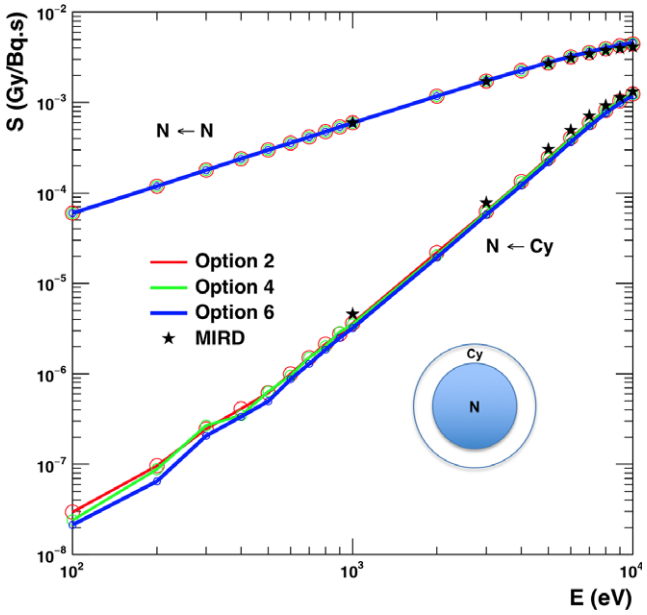

FIG. 6. S-values for the nucleus ← nucleus (denoted as "N ← N") and the nucleus ← cytoplasm (denoted as "N ← Cy") configurations, in a simplified spherical cell (nucleus of radius 4 microns and cytoplasm of thickness 1 micron — as shown in the inset), as a function of incident electron energy in liquid water simulated using the "svalue" example, for the three Geant4-DNA constructors (colored circles). MIRD calculations are indicated as well (black stars).[87]

1 μm. These data were generated by shooting monoenergetic electrons randomly (in position and in direction) from the cytoplasm or from the nucleus. Results are presented for the nucleus as target: either for the (nucleus ← nucleus) configuration (upper curves) or for the (nucleus ← cytoplasm) configuration (lower curves), up to 10 keV, the maximum common high-energy limit of physics constructors. Inspection of this figure illustrates a very good agreement between physics constructors. For the configuration where the nucleus is the source, "option 4" differs from "option 2" by less than 1% over the whole energy range and "option 6" differs from "option 2" by less than 1% up to 5 keV and remain below 5% above this energy. Regarding the configuration where the cytoplasm is the source, differences are larger especially for the lowest incident energies: "option 4" differs from "option 2" by less than 5% down to 3 keV and "option 6" differs from "option 2" by less than 10% down to about 4 keV. This overall agreement between Geant4-DNA constructors has been previously observed when studying the distribution of energy deposition in small spheres of liquid water larger than a few hundreds of nanometers in diameter.[60] S-values for these two configurations have been calculated by the MIRD Committee[87] and are also shown in Fig. 6. Regarding the (nucleus ← nucleus) configuration, deviations between the three Geant4-DNA physics constructors and MIRD values are less than 10%, up to about 10 keV. Larger deviations are observed for the (nucleus ← cytoplasm) configuration, especially for the lowest energies, reaching at most 9% at 10 keV and at most 30% at 1 keV both for "option 6". These deviations from MIRD have been already observed, as we

presented in Ref. [74]. The public version of this example included in Geant4 10.4 calculates S-values for a single target sphere, whereas the version of this example described in this work will be released in the near future.

3.G. The "slowing" example

3.G.1. Purpose

This example can be used for the simulation of slowing-down spectra of electrons in liquid water. This is another application that is regularly used to compare TS codes.[89] Such spectra represent the fluence distribution (differential in energy) of both the primary and all subsequent generations of secondary electrons generated through the full slowing-down process of the incident particle.[72] The user can activate all atomic de-excitation processes as well as inelastic subexcitation processes for electrons (vibrational excitation and molecular attachment), as these impact the spectra shape. A tracking cut can also be applied. The simulated slowing-down spectra are expressed as $1/(cm^2.eV.Gy)$.

3.G.2. Results and discussion

Figure 7 presents the simulation of electron slowing-down spectra in liquid water for 100 eV, 1 keV, and 10 keV incident monoenergetic electrons, all simulated with the "slowing" example. In these simulations, the elastic scattering process was not considered, except for "option 6" where elastic scatterings are accompanied by small energy losses, as explained in Ref. [48]. Similar results were obtained for "option 2" and "option 4" as we previously described in Ref. [72]: for the 100 eV and 1 keV incident energies, "option 4" values are slightly larger than "option 2" values, down to about 15 eV. This is caused by the lower stopping power values of "option 4" compared to "option 2" (see Fig. 3 left panel of this work). "Option 6" values appear systematically lower than the two other constructors. This is similarly caused by the stopping power values of "option 6" which are larger than the two other constructors (see Fig. 3, left panel). The influence of Auger electron production can be observed for all three constructors at the production threshold (around 500 eV) on the 10 keV spectra.

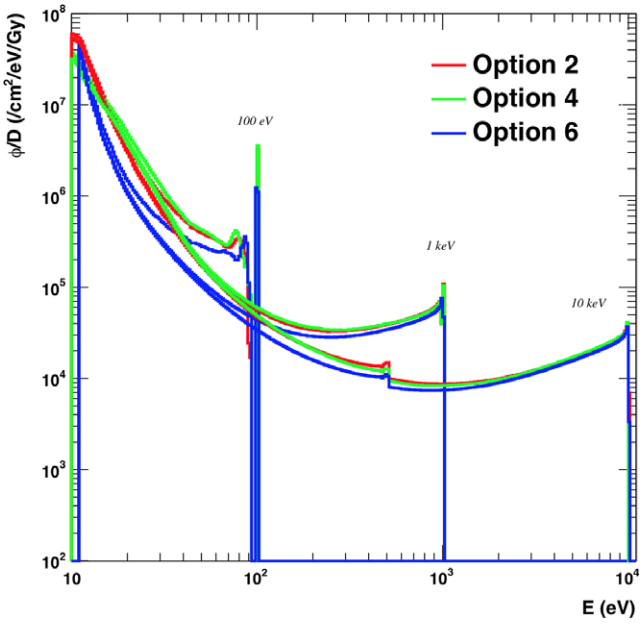

FIG. 7. Slowing-down spectra in liquid water for 100 eV, 1 keV, and 10 keV monoenergetic electrons simulated with the "slowing" example using the three Geant4-DNA physics constructors.

3.H. The "microyz" example

3.H.1. Purpose

The "microyz" example is mainly useful for simulations in microdosimetry,[90] a formalism largely used for the investigation of biological effects of ionizing radiation at the cellular level (where typical dimensions are of the order of a few microns). It was mainly developed to explain to users how to simulate microdosimetry spectra of lineal energy (usually denoted as "y") and specific energy (usually denoted as "z"), thus the example name "microyz" and their related quantities (frequency-mean and dose-mean averages) in small spheres of liquid water. This example applies a weighting procedure avoiding bias of energy scoring in regions of the full cascade of particles with large number of energy depositions, and is described more fully in other work.[60] Users have the possibility to apply a tracking cut. Lineal energies (in eV/nm) and specific energies (in Gy) are simulated for each incident particle. Corresponding mean values can be calculated using the provided ROOT macro file.

3.H.2. Results and discussion

Performance of the "microyz" extended example has been described in detail in our previous publication (Ref. [60]). As another illustration, we present in Fig. 8 the frequency-mean lineal energy distribution of electrons as a function of their incident kinetic energy, obtained in a 2- and 100-nm-diameter scoring sphere, for an incident statistics of 10^6 electrons. In order to adopt our previous simulation conditions described in Ref. [60], vibrational excitation and attachment have not been considered for "option 2". Default tracking cuts have been used for "option 4" (10 eV) and "option 6" (11 eV). A tracking cut of 9 eV (instead of the default value of 7.4 eV) has been used for "option 2", since no energy loss process occurs below 9 eV when vibrational excitation and attachment are not considered (as it is the case in the present simulations).

For the 2-nm sphere, frequency-mean lineal energies obtained with "option 2" and "option 4" constructors are very similar (they differ by less than 10% over the whole energy range), while "option 6" values are systematically

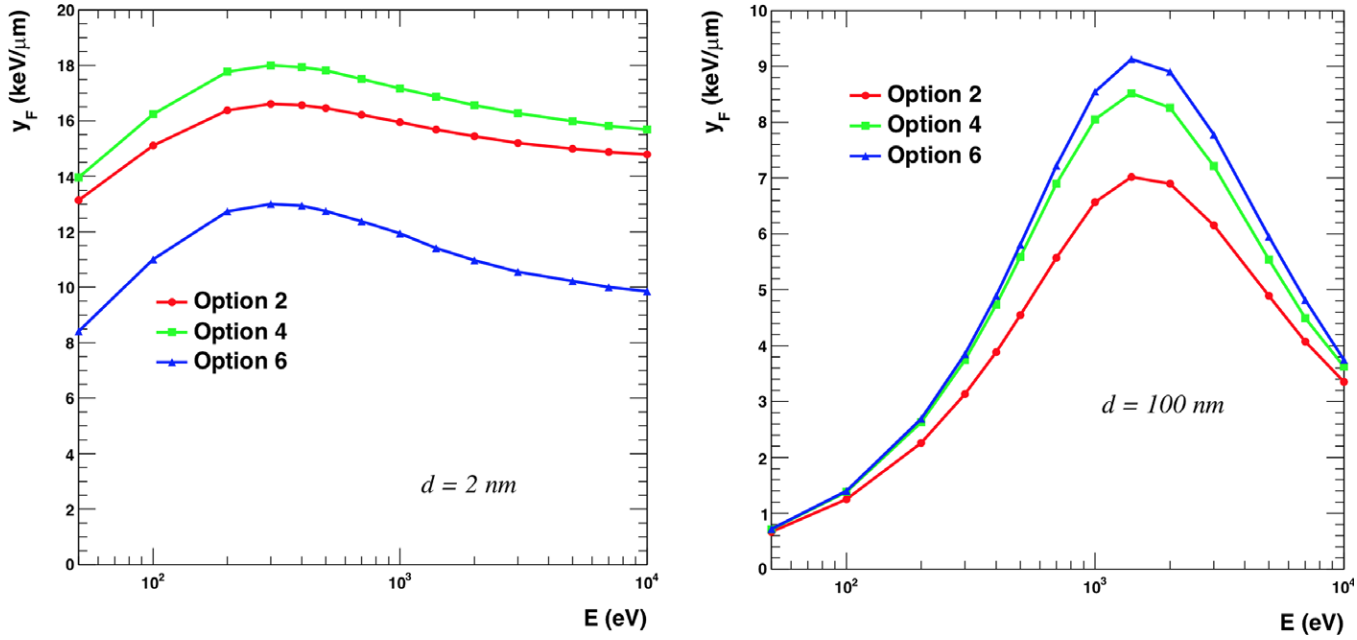

FIG. 8. Frequency-mean lineal energy (y_F) as a function of incident electron kinetic energy for a scoring sphere of diameter 2 nm (left panel) and 100 nm (right panel). These distributions have been simulated with the "microyz" example for the three Geant4-DNA physics constructors.

lower by 22% to 36%. This large discrepancy is caused by the numerous very small energy losses occurring during elastic scattering in "option 6" as we explained in Ref. [60] and which are accounted for in the calculation of lineal energy values. As an illustration, at 200 eV, when energy losses are not considered during elastic scattering of "option 6", 100% of total energy deposits scored in spheres are larger than 8 eV; on the contrary, when these small energy losses are considered (which is the default setting of "option 6"), about 30% of such deposits are less than 8 eV down to the microeV scale, resulting in a lower frequency-mean lineal energy at this energy, as observed in the left panel of Fig. 8. For the 100 nm sphere, although frequency-mean lineal energies have similar trend as a function of incident energy, the values obtained for "option 6" are larger than for "option 4", the latter being larger than the "option 2" values. Compared to "option 2" values, "option 6" are larger by 7% (at 50 eV) up to 30% (at 1 keV), and "option 4" values are larger by 7% at 50 eV up to 24% at 700 eV. The dominance of "option 6" values over the two other sets results from the larger inelastic cross sections of "option 6", while these cross sections are in closer agreement for "option 2" and "option 4" (see Fig. 4 of Ref. [6]).

3.I. The "TestEm12" example

3.I.1. Purpose

This example has not been specifically developed for Geant4-DNA. It is a reference example which can be used with all Geant4 electromagnetic physics models. We recently added the possibility to also use Geant4-DNA physics constructors and a macro file allowing the simulation of dose point kernels (DPK) using these constructors. DPKs serve particularly as benchmarks for the accuracy of electron elastic and inelastic scattering models, as has been previously demonstrated by our Collaboration in Ref. [75]. Energy deposition is recorded in virtual spherical shells around the emission point source and the user can easily select the number of shells using this macro file. Simulated DPK spectra are expressed in MeV/mm as a function of the distance in nm from the point source.

3.I.2. Results and discussion

An extensive verification of DPK distributions has been recently described in Ref. [75], where "option 2," "option 4," and "option 6" physics constructors have been compared. We show in Fig. 9 the DPK obtained for 100 eV and 1 keV incident monoenergetic electrons, using these three constructors with their default tracking cut. We also present DPKs obtained for "option 2" (dashed lines) in the case where inelastic subexcitation processes (vibrational excitation and attachment) are not considered (these processes are not included in the "option 4" and "option 6" constructors — see Table I). In all cases, DPKs obtained with "option 2" are more diffusive than the two other constructors (longer tail toward large radius values). At 100 eV, this behavior is clearly magnified when inelastic subexcitation processes for "option 2" are ignored (dashed red line). This is a direct result of the much lower excitation cross section of "option 2" in comparison to "option 4" and "option 6".[59] At 1 keV, "option 6" is less diffusive and presents a larger maximum than "option 2" (16% larger and about 4 nm closer to the source) and "option 4" (12% larger and about 4 nm closer to

the source). The observed trend (less diffusive DPKs for "option 6" than for the two other constructors) follows the behavior of the total mean free path (which considers elastic and inelastic interactions) as a function of incident energy shown in Fig. 4, underlining that models with longer total mean free path lead to more diffusive DPKs. The observed larger maximum of "option 6" is closer to the predictions of the PENELOPE-2011 Monte Carlo code[29] used in a step by step mode in the 1 keV–10 keV range. The reader is invited to refer to Ref. [75] for more detail regarding the comparison of Geant4-DNA DPKs with the PENELOPE code in this 1 keV–10 keV energy range.

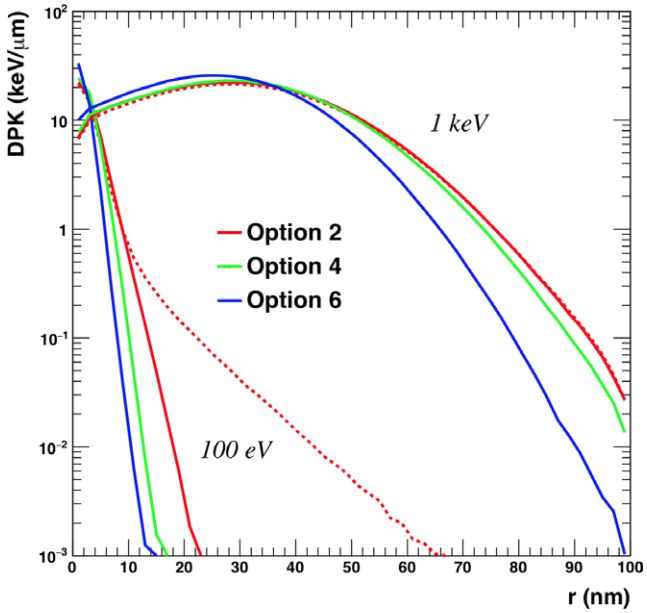

FIG. 9. Dose point kernels (DPK) for 10^6 monoenergetic electrons of 100 eV and 1 keV in liquid water, simulated using the "TestEm12" extended example. Results are shown for the three Geant4-DNA physics constructors. The red dashed lines show "option 2" DPKs when inelastic subexcitation processes (vibrational excitation and attachment) are not taken into account.

3.J. The "TestEm5" example

3.J.1. Purpose

"TestEm5" is another Geant4 electromagnetic physics example, which can be used to investigate atomic relaxation. This includes the production of fluorescence photons or Auger electrons after removal of an atomic electron induced by ionization, the photoelectric effect or Compton scattering processes. This example was used to illustrate the recent addition[52] of Auger cascade simulation in Geant4 electromagnetic physics. Moreover, it has been updated in order to demonstrate how to mark fluorescence photons and Auger electrons generated from the atomic relaxation cascade induced by the Geant4-DNA ionization processes. Using a dedicated macro file that fully activates atomic relaxation — including Auger cascades — without any cut for the production of relaxation products, Geant4-DNA users can now easily score the kinetic energy of these particles in histograms.

3.J.2. Results and discussion

Figure 10 (left panel) illustrates the possibility to detect Auger electrons initiated by the Geant4-DNA ionization

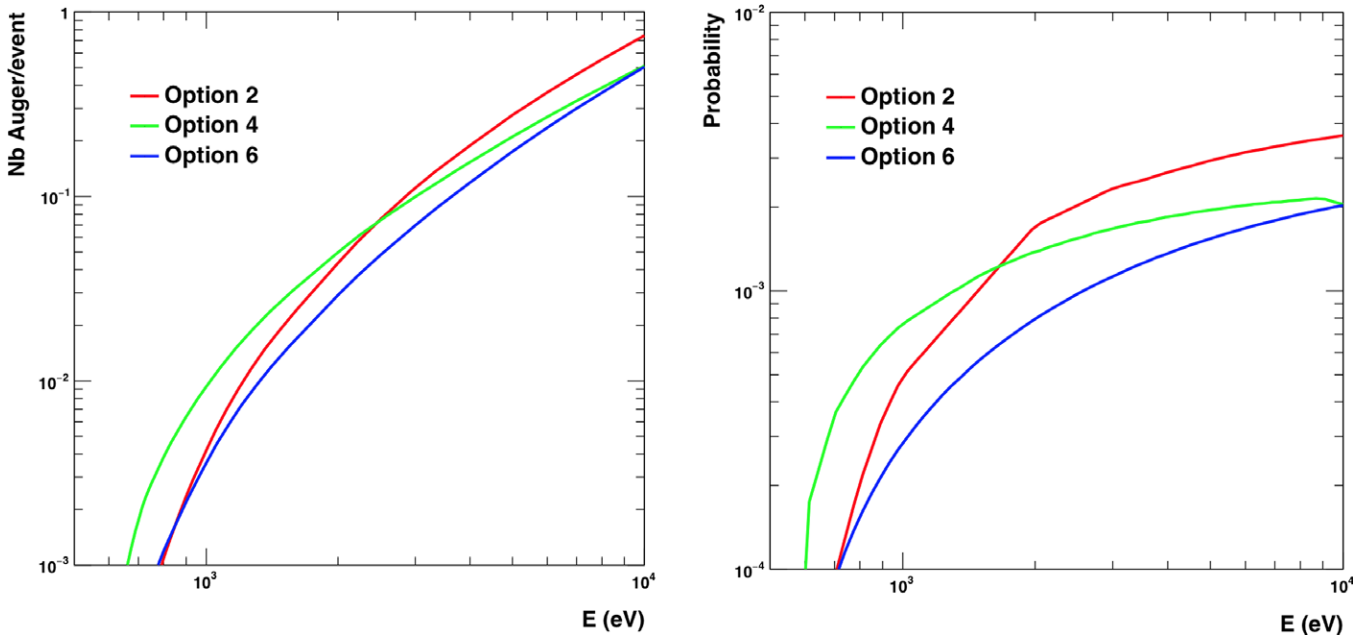

FIG. 10. The left panel shows the number of Auger electrons generated per incident electron by the Geant4-DNA ionization process for the three physics constructors as a function of incident electron kinetic energy. The right panel shows the probability of K-shell ionization of each constructor as a function of incident electron kinetic energy.

process: the number of Auger electrons per incident electron is presented as a function of electron kinetic energy. Auger electrons are generated from the ionized oxygen atom of the water molecule with energies and frequencies tabulated in the EADL database.[51] The three constructors show similar behavior with "option 2" leading to larger production rates compared to "option 4" and "option 6" above 2 keV. For example, at 10 keV, the production of Auger electrons by "option 2" is about 50% larger to "option 4" and "option 6". On the contrary, at low energy, the production is larger for "option 4" than for the two other constructors. For example, at 1 keV, "option 4" produces about 120% more Auger electrons than "option 2" and about 160% more than "option 6". The trends of these rates as a function of energy result from the probability of electron-impact ionization of the K-shell in oxygen atoms, which depend on the modeling of the ionization process. This probability is represented for a single electron on the right panel of Fig. 10 for the three constructors, as a function of the electron energy. It has been calculated as the probability that the incident electron undergoes impact ionization (among the ionization, excitation, and elastic scattering processes, and using the corresponding cross sections) multiplied by the probability that the ionization occurs on the K-shell (among the five shells of the water molecule). The probability obtained with "option 2" is larger than for the two other constructors at high energy, while "option 4" dominates below 1 keV, in agreement with the trends observed in the left panel of Fig. 10.

4. CONCLUSION

In this work we have reviewed all Geant4-DNA example applications available as part of Geant4 version 10.4 (and some examples soon to be released), for the simulation of track structures in liquid water. This is, to the best knowledge of the authors, the first time that such a variety of examples for TS simulations are made freely available to the community. In addition to their pedagogical role, these examples also serve for evaluating Geant4-DNA physics models' performance and their evolution over time (regression testing). In particular, we have underlined in this work the performance of the recent "option 4" and "option 6" Geant4-DNA physics constructors — developed at Ioannina University (in Greece) and at Paul Sabatier University (in France), respectively — compared to the alternative default constructor "option 2". We have shown that on one hand the "option 6" stopping powers for electrons in liquid water are somewhat closer to the recent ICRU90 recommendations than "option 4" and give larger and less diffusive DPKs, as also predicted by the PENELOPE Monte Carlo code. One should, however, underline that the less diffusive DPKs predicted by PENELOPE also result from the larger tracking cut of PENELOPE (50 eV vs 7.4 eV for "option 2," 10 eV for "option 4," and 11 eV for "option 6"). On the other hand, "option 4" predicts W-values closer to other Monte Carlo simulations and experimental data in the gas phase than "option 6". In the absence of low-energy validation data (<1 keV) in liquid water, it remains difficult to give a firm recommendation for a specific constructor. However, the usage of these recent constructors could be useful for evaluating quantitatively the dependence of simulation results on such physics models in any user application. In addition to this lack of experimental validation, users should keep in mind that Geant4-DNA (similar to other TS codes) assumes the classical trajectory approximation, which becomes gradually less valid at low energies (especially below 20–50 eV). Such limitations are discussed in detail by Thomson et al.[91] and Liljequist et al.[92] Although it was already shown[47] that "option 4" constructor improves upon "option 2" at various track structure simulations at sub-keV energies, the latter is still used since it covers a larger energy range up to 1 MeV ("option 4" has an upper limit of 10 keV and "option 6" of 256 keV). The "option 4" constructor will soon be extended to relativistic energies, benefiting notably from newly available experimental data and theoretical calculations,[83,93] which will extend its usage to a variety of applications beyond 10 keV. These examples will then be used to quantify the impact of such extended models on TS simulations. Regarding the inclusion of cross sections for other materials than liquid water (in particular DNA components or precursors), new cross sections allowing the transport of electrons down to 12 eV and protons used as projectiles (in the range 70 keV–10 MeV) extracted from Ref. [10] have also been included in the Geant4 10.4 release. Their use and validation will be described in a future publication. Moreover, the addition of such other biological materials in the "option 6" constructor as implemented in the CPA100 code, is also planned.

ACKNOWLEDGMENTS

The Geant4-DNA Collaboration acknowledges the following sources of funding and support: the French National Center for Scientific Research (CNRS) Projet International de Coopération Scientifique (PICS) #7340 France–Greece (2016–2018), the University of Bordeaux Initiative of Excellence–France–International Postdoctorates program in the framework of the "France-Japan Particle Physics Laboratory" International Associated Laboratory (2016–2017) and the University of Bordeaux Initiative of Excellence–France–International Doctorates program in the framework of the "France-Korea Particle Physics Laboratory" International Associated Laboratory (2016–2019). M. A. Bernal acknowledges the support received from the Conselho Nacional para o Desenvolvimento Cientıfico e Tecnologico (CNPq) and FAPESP foundation, in Brazil, for financing his research activities through the projects 306775/2015-8 and 2011/51594-2, respectively. S. Guatelli and D. Sakata acknowledge the financial support of the Australian Research Council, ARC DP170100967. I. Kyriakou acknowledges financial support from European Space Agency (Contract No. 4000112863/14/NL/HB).

CONFLICT OF INTEREST

The authors have no conflicts to disclose.

[*]Present address: University of Bordeaux, CENBG, UMR 5797, F-33170 Gradignan, France

[#]Present address: CNRS, IN2P3, CENBG, UMR 5797, F-33170 Gradignan, France

[a)]Author to whom correspondence should be addressed. Electronic mail: incerti@cenbg.in2p3.fr.

REFERENCES

1. El Naqa I, Pater P, Seuntjens J. Monte Carlo role in radiobiological modelling of radiotherapy outcomes. *Phys Med Biol*. 2012;57: R75–R97.
2. Friedland W, Schmitt E, Kundrát P, et al. Comprehensive track-structure based evaluation of DNA damage by light ions from radiotherapy-relevant energies down to stopping. *Sci Rep*. 2017;7:45161.
3. Nikjoo H, Emfietzoglou D, Liamsuwan T, Taleei R, Liljequist D, Uehara S. Radiation track, DNA damage and response—a review. *Rep Prog Phys*. 2016;79:116601.
4. Incerti S, Baldacchino M, Bernal M, et al. The Geant4-DNA Project. *Int J Model Simul Sci Comput*. 2010;01:157–178.
5. Incerti S, Ivanchenko A, Karamitros M, et al. Comparison of GEANT4 very low energy cross section models with experimental data in water. *Med Phys*. 2010;37:4692–4708.
6. Bernal MA, Bordage MC, Brown JMC, et al. Track structure modeling in liquid water: a review of the Geant4-DNA very low energy extension of the Geant4 Monte Carlo simulation toolkit. *Phys Med*. 2015;31:861–874.
7. Agostinelli S, Allison J, Amako K, et al. Geant4 - a simulation toolkit. *Nucl Instrum Meth A*. 2003;506:250–303.
8. Allison J, Amako K, Apostolakis H, et al. Geant4 developments and applications. *IEEE Trans Nucl Sci*. 2006;53:270–278.
9. Allison J, Amako K, Apostolakis J, et al. Recent developments in Geant4. *Nucl Instrum Meth A*. 2016;835:186–225.
10. Bug MU, Yong Baek W, Rabus H, Villagrasa C, Meylan S, Rosenfeld AB. An electron-impact cross section data set (10 eV–1 keV) of DNA constituents based on consistent experimental data: a requisite for Monte Carlo simulations. *Rad Phys Chem*. 2017;130:459–479.
11. Karamitros M, et al. Diffusion-controlled reactions modeling in Geant4-DNA. *J Comput Phys*. 2014;274:841–882.
12. Incerti S, Douglass M, Penfold S, Guatelli S, Bezak E. Review of Geant4-DNA applications for micro and nanoscale simulations. *Phys Med*. 2016;32:1187–1200.
13. Lampe N. The long term impact of ionising radiation on living systems. PhD thesis, Université Clermont Auvergne; 2017.
14. Lampe N, Karamitros M, Breton V, et al. Mechanistic DNA damage simulations in Geant4-DNA part 1: a parameter study in a simplified geometry. *Phys Med*. 2018;48:135–145.
15. Lampe N, Karamitros M, Breton V, et al. Mechanistic DNA damage simulations in Geant4-DNA Part 2: electron and proton damage in a bacterial cell. *Phys Med*. 2018;48:146–155.
16. Meylan S, Incerti S, Karamitros M, et al. Simulation of early DNA damage after the irradiation of a fibroblast cell nucleus using Geant4-DNA. *Sci Rep*. 2017;7:11923.
17. Nikjoo H, Taleei R, Liamsuwan T, Liljequist D, Emfietzoglou D. Perspectives in radiation biophysics: from radiation track structure simulation to mechanistic models of DNA damage and repair. *Rad Phys Chem*. 2016;128:3–10.
18. Dingfelder M, Jorjishvili IG, Gersh JA, Toburen LH. Heavy ion track structure simulations in liquid water at relativistic energies. *Rad Prot Dos*. 2006;122:26–27.
19. Nikjoo H, Emfietzoglou D, Watanabe R, Uehara S. Can Monte Carlo track structure codes reveal reaction mechanism in DNA damage and improve radiation therapy? *Rad Phys Chem*. 2008;77:1270–1279.
20. Siantar CLH, et al. Description and dosimetric verification of the PEREGRINE Monte Carlo dose calculation system for photon beams incident on a water phantom. *Med Phys*. 2001;28:1322–1337.
21. Strigari L, Menghi E, D'Andrea M, Benassi M. Monte Carlo dose voxel kernel calculations of beta-emitting and Auger-emitting radionuclides for internal dosimetry: a comparison between EGSnrcMP and EGS4. *Med Phys*. 2006;33:3383–3389.
22. Lehmann J, et al. Monte Carlo treatment planning for molecular targeted radiotherapy within the MINERVA system. *Phys Med Biol*. 2005;50:947–958.
23. Falzone N, Fernández-Varea JM, Flux G, Vallis KA. Monte Carlo evaluation of auger electron-emitting theranostic radionuclides. *J Nucl Med*. 2015;56:1441–1446.
24. Bousis C, Emfietzoglou D, Nikjoo H. Monte Carlo single-cell dosimetry of I-131, I-125 and I-123 for targeted radioimmunotherapy of B-cell lymphoma. *Int J Radiat Biol*. 2012;88:908–915.
25. Carlson DJ, Stewart RD, Semenenko VA, Sandison GA. Combined use of Monte Carlo DNA damage simulations and deterministic repair models to examine putative mechanisms of cell killing. *Rad Res*. 2008;169:447–459.
26. Semenenko VA, Stewart RD, Ackerman EJ. Monte Carlo simulation of base and nucleotide excision repair of clustered DNA damage sites. I. Model properties and predicted trends. *Rad Res*. 2005;164: 180–193.
27. Nikjoo H, Uehara S, Emfietzoglou D, Cucinotta F. Track-structure codes in radiation research. *Rad Meas*. 2006;41:1052–1074.
28. Kawrakow I, Mainegra-Hing E, Rogers DWO, Tessier F, Walters PRB. The EGSnrc Code System: Monte Carlo Simulation of Electron and Photon Transport. NRCC Report PIRS-701; 2017.
29. Baró J, Sempau J, Fernández-Varea JM, Salvat F. PENELOPE: an algorithm for Monte Carlo simulation of the penetration and energy loss of electrons and positrons in matter. *Nucl Instrum Meth B*. 1995;100:31–46.
30. Briesmeister JF. *MCNP-A General Monte Carlo Code for Neutron and Photon Transport*. LA-7396-M 3A. Los Alamos: Los Alamos National Laboratory; 1986.
31. Ferrari A, Sala PR, Fasso A, Ranft J. *FLUKA: A Multi-Particle Transport Code (Program version 2005)*. Geneva: CERN; 2005.
32. Fernández-Varea JM, González-Muñoz G, Galassi ME, et al. Limitations (and merits) of PENELOPE as a track-structure code. *Int J Radiat Biol*. 2012;88:66–70.
33. Dingfelder M, Ritchie RH, Turner JE, Friedland W, Paretzke HG, Hamm RN. Comparisons of calculations with PARTRAC and NOREC: transport of electrons in liquid water. *Rad Res*. 2008;169:584–594.
34. Friedland W, Dingfelder M, Kundrát P, Jacob P. Track structures, DNA targets and radiation effects in the biophysical Monte Carlo simulation code PARTRAC. *Mutat Res*. 2011;711:28–40.
35. Liamsuwan T, Emfietzoglou D, Uehara S, Nikjoo H. Microdosimetry of low-energy electrons. *Int J Radiat Biol*. 2012;88:899–907.
36. Taleei R, Nikjoo H. Repair of the double-strand breaks induced by low energy electrons: a modelling approach. *Int J Radiat Biol*. 2012;88:948–953.
37. Taleei R, Girard PM, Sankaranarayanan K, Nikjoo H. The non-homologous end-joining (NHEJ) mathematical model for the repair of double-strand breaks: II. Application to damage induced by ultrasoft x rays and low-energy electrons. *Rad Res*. 2013;179:540–548.
38. Goorley JT, James MR, Booth TE, et al. Initial MCNP6 Release Overview - MCNP6 version 1.0, United States 2013-06-26; 2013.
39. McNamara AL, Geng C, Turner R, et al. Validation of the radiobiology toolkit TOPAS-nBio in simple DNA geometries. *Phys Med*. 2017;33:207–215.
40. Pham QT, et al. Coupling of Geant4-DNA physics models into the GATE Monte Carlo platform: evaluation of radiation-induced damage for clinical and preclinical radiation therapy beams. *Nucl Instrum Meth B*. 2015;353:46–55.
41. Dingfelder M. Updated model for dielectric response function of liquid water. *Appl Radiat Isot*. 2014;83:142–147.
42. Emfietzoglou D, Kyriakou I, Abril I, Garcia-Molina R, Nikjoo H. Inelastic scattering of low-energy electrons in liquid water computed from optical-data models of the Bethe surface. *Int J Radiat Biol*. 2012;88:22–28.

43. Fernandez-Varea J, Salvat F, Dingfelder M, Liljequist D. A relativistic optical-data model for inelastic scattering of electrons and positrons in condensed matter. *Nucl Instrum Meth B*. 2005;229:187–218.
44. Tran HN, et al. Modeling proton and alpha elastic scattering in liquid water in Geant4-DNA. *Nucl Instrum Meth B*. 2015;343:132–137.
45. Francis Z, Incerti S, Ivanchenko V, et al. Monte Carlo simulation of energy-deposit clustering for ions of the same LET in liquid water. *Phys Med Biol*. 2012;57:209–224.
46. Cullen SE, Hubbell JH, Kissel L. *EPDL97: The Evaluated Photon Data Library, 97 Version*, Vol UCRL-LR-50400-V6-R5. Livermore: Lawrence Livermore National Laboratory; 1997.
47. Kyriakou I, Incerti S, Francis Z. Technical note: improvements in GEANT4 energy-loss model and the effect on low-energy electron transport in liquid water. *Med Phys*. 2015;42:3870–3876.
48. Bordage MC, Bordes J, Edel S, et al. Implementation of new physics models for low energy electrons in liquid water in Geant4-DNA. *Phys Med*. 2016;32:1833–1840.
49. Michaud M, Wen A, Sanche L. Cross sections for low-energy (1–100 eV) electron elastic and inelastic scattering in amorphous ice. *Rad Res*. 2003;159:3–22.
50. Melton CE. Cross sections and interpretation of dissociative attachment reactions producing OH−, O−, and H− in H2O. *J Chem Phys*. 1972;57:4218–4225.
51. Perkins ST, Cullen D, Chen M, Rathkopf J, Scofield J, Hubbell J. *Tables and Graphs of Atomic Subshell and Relaxation Data Derived From the LLNL Evaluated Atomic Data Library (EADL), Z = 1-100*, Vol UCRL-50400-V30. Livermore: Lawrence Livermore National Laboratory; 1991.
52. Incerti S, Suerfu B, Xu J, et al. Simulation of Auger electron emission from nanometer-size gold targets using the Geant4 Monte Carlo simulation toolkit. *Nucl Instrum Meth B*. 2016;372:91–101.
53. Mantero A, Ben Abdelouahed H, Champion C, et al. PIXE simulation in Geant4. *X-Ray Spec*. 2011;40:135–140.
54. Emfietzoglou D. Inelastic cross-sections for electron transport in liquid water: a comparison of dielectric models. *Radiat Phys Chem*. 2003;66:373–385.
55. Emfietzoglou D, Nikjoo H. The effect of model approximations on single-collision distributions of low-energy electrons in liquid water. *Rad Res*. 2005;163:98–111.
56. Rudd M, Kim Y-K, Märk T, Schou J, Stolterfoht N, Toburen L. Secondary electron spectra from charged particle interactions. ICRU Report 55; 1996.
57. Champion C, Incerti S, Aouchiche H, Oubaziz D. A free-parameter theoretical model for describing the electron elastic scattering in water in the Geant4 toolkit. *Radiat Phys Chem*. 2009;78:745–750.
58. Francis Z, Incerti S, Capra R, et al. Molecular scale track structure simulations in liquid water using the Geant4-DNA Monte-Carlo processes. *Appl Radiat Isot*. 2011;69:220–226.
59. Kyriakou I, Šefl M, Nourry V, Incerti S. The impact of new Geant4-DNA cross section models on electron track structure simulations in liquid water. *J Appl Phys*. 2016;119:194902.
60. Kyriakou I, Emfietzoglou D, Ivanchenko V, et al. Microdosimetry of electrons in liquid water using the low-energy models of Geant4. *J Appl Phys*. 2017;122:024303.
61. Emfietzoglou D, Kyriakou I, Garcia-Molina R, Abril I. Inelastic mean free path of low-energy electrons in condensed media: beyond the standard models. *Surf Interface Anal*. 2017;49:4–10.
62. Emfietzoglou D, Cucinotta FA, Nikjoo H. A complete dielectric response model for liquid water: a solution of the bethe ridge problem. *Radiat Res*. 2005;164:202–211.
63. Emfietzoglou D, Kyriakou I, Garcia-Molina R, Abril I, Nikjoo H. Inelastic cross sections for low-energy electrons in liquid water: exchange and correlation effects. *Radiat Res*. 2013;180:499–513.
64. Emfietzoglou D, Kyriakou I, Garcia-Molina R, Abril I. The effect of static many-body local-field corrections to inelastic electron scattering in condensed media. *J Appl Phys*. 2013;114:144907.
65. Uehara S, Nikjoo H, Goodhead DT. Cross-sections for water vapour for the Monte Carlo electron track structure code from 10 eV to the MeV region. *Phys Med Biol*. 1993;38:1841–1858.
66. Aouchiche H, Champion C, Oubaziz D. Electron and positron elastic scattering in gaseous and liquid water: a comparative study. *Radiat Phys Chem*. 2008;77:107–114.
67. Terrissol M, Beaudré A. Simulation of space and time evolution of radiolytic species induced by electrons in water. *Radiat Prot Dos*. 1990;31:175–177.
68. Dingfelder M, Hantke D, Inokuti M, Paretzke HG. Electron inelastic-scattering cross sections in liquid water. *Radiat Phys Chem*. 1999;53:1–18.
69. Kim Y-K, Rudd ME. Binary-encounter-dipole model for electron-impact ionization. *Phys Rev A*. 1994;50:3954–3967.
70. Apostolakis J, Asai M, Bagulya A, et al. Progress in Geant4 electromagnetic physics modelling and validation. *J Phys Conf Ser*. 2015;664:072021.
71. Ivanchenko VN, Kadri O, Maire M, Urban L. Geant4 models for simulation of multiple scattering. *J Phys Conf Ser*. 2010;219:032045.
72. Incerti S, Kyriakou I, Tran HN. Geant4-DNA simulation of electron slowing-down spectra in liquid water. *Nucl Instrum Meth B*. 2017;397:45–50.
73. André T, et al. Comparison of Geant4-DNA simulation of S-values with other Monte Carlo codes. *Nucl Instrum Meth B*. 2014;319:87–94.
74. Šefl M, Incerti S, Papamichael G, Emfietzoglou D. Calculation of cellular S-values using Geant4-DNA: the effect of cell geometry. *Appl Radiat Isot*. 2015;104:113–123.
75. Bordes J, Incerti S, Lampe N, Bardiès M, Bordage M-C. Low-energy electron dose-point kernel simulations using new physics models implemented in Geant4-DNA. *Nucl Instrum Meth B*. 2017;398:13–20.
76. Brun R, Rademakers F. ROOT — an object oriented data analysis framework. *Nucl Instrum Meth A*. 1997;389:81–86.
77. Brown JMC, Dimmock MR, Gillam JE, Paganin DM. A low energy bound atomic electron compton scattering model for Geant4. *Nucl Instrum Meth B*. 2014;338:77.
78. Friedland W, Jacob P, Bernhardt P, Paretzke HG, Dingfelder M. Simulation of DNA damage after proton irradiation. *Radiat Res*. 2003;159:401–410.
79. Seltzer S, Fernández-Varea J, Andreo P, et al. Key data for ionizing-radiation dosimetry: measurement standards and applications, ICRU Report 90; 2016.
80. Uehara S, Toburen L, Nikjoo H. Development of a Monte Carlo track structure code for low-energy protons in water. *Int J Radiat Biol*. 2001;77:139–154.
81. Francis Z, Incerti S, Karamitros M, Tran HN, Villagrasa C. Stopping power and ranges of electrons, protons and alpha particles in liquid water using the Geant4-DNA package. *Nucl Instrum Meth B*. 2011;269:2307–2311.
82. Emfietzoglou D, Nikjoo H. Accurate electron inelastic cross sections and stopping powers for liquid water over the 0.1–10 keV range based on an improved dielectric description of the bethe surface. *Radiat Res*. 2007;167:110–120.
83. Emfietzoglou D, Papamichael G, Nikjoo H. Monte Carlo electron track structure calculations in liquid water using a new model dielectric response function. *Radiat Res*. 2017;188:355–368.
84. Plante I, Cucinotta FA. Cross sections for the interactions of 1 eV–100 MeV electrons in liquid water and application to Monte-Carlo simulation of HZE radiation tracks. *New J Phys*. 2009;11:063047.
85. Combecher D. Measurement of W values of low-energy electrons in several gases. *Radiat Res*. 1980;84:189–218.
86. Semenenko VA, Turner JE, Borak TB. NOREC, a Monte Carlo code for simulating electron tracks in liquid water. *Radiat Environ Biophys*. 2003;42:213–217.
87. Goddu SM, Howell R, Bouchet L, Bolch W, Rao DV. *MIRD Cellular S Values: Self-Absorbed Dose Per Unit Cumulated Activity for Selected Radionuclides and Monoenergetic Electron and Alpha Particle Emitters Incorporated into Different Cell Compartments*. Reston VA, USA: Society of Nuclear Medicine; 1997.
88. Uusijärvi H, Bernhardt P, Ericsson T, Forssell-Aronsson E. Dosimetric characterization of radionuclides for systemic tumor therapy: influence of particle range, photon emission, and subcellular distribution. *Med Phys*. 2006;33:3260–3269.
89. Vassiliev ON. Electron slowing-down spectra in water for electron and photon sources calculated with the Geant4-DNA code. *Phys Med Biol*. 2012;57:1087–1094.
90. Rossi HH, Zaider M. *Microdosimetry and Its Applications*. Berlin: Springer; 1996.

91. Thomson RM, Kawrakow I. On the Monte Carlo simulation of electron transport in the sub-1 keV energy range. *Med Phys*. 2011;38: 4531–4544.
92. Liljequist D, Nikjoo H. On the validity of trajectory methods for calculating the transport of very low energy (<1 keV) electrons in liquids and amorphous media. *Radiat Phys Chem*. 2014;99:45–52.
93. Hayashi H, Hiraoka N. Accurate measurements of dielectric and optical functions of liquid water and liquid benzene in the VUV region (1–100 eV) using small-angle inelastic x-ray scattering. *J Phys Chem B*. 2015;119:5609–5623.

SUPPORTING INFORMATION

Additional supporting information may be found online in the Supporting Information section at the end of the article

Fig. S1. Single tracks of a 1 MeV proton (left track), a 4 MeV alpha particle (middle track) and a 12 MeV carbon ion (right track) in liquid water simulated using "dnaphysics" and the G4EmDNAPhysicsActivator interface. Each colored dot corresponds to a physical interaction. We used the same color scheme as in Figure 1. Tracks are shown on a restricted length of 500 nm. The dominance of green dots underlines the frequent elastic scatterings.

Table S1. Description of the automatic combination of Geant4-DNA models with Geant4 standard electromagnetic models for liquid water, performed by the "G4EmDNAPhysicsActivator" interface available from Geant4 10.4 release (December 2017), and illustrated in the "dnaphysics" example. ($^{+}$) Photon models origin from the "low energy electromagnetic physics" set of models of Geant4.[9,77]